CHROMOSPHERIC HEIGHT AND DENSITY MEASUREMENTS IN A SOLAR FLARE OBSERVED WITH RHESSI

I. *Theory*

JOHN C. BROWN[1], MARKUS J. ASCHWANDEN[2] and EDUARD P. KONTAR[1]
[1]*Astronomy and Astrophysics Group, Dept. of Physics and Astronomy, University of Glasgow, Glasgow G12 8QQ, U.K. (e-mail: john@astro.gla.ac.uk)*
[2]*Lockheed Martin Advanced Technology Center, Solar & Astrophysics Laboratory, Dept. L9-41, Bldg.252, 3251 Hanover St., Palo Alto, CA 94304, U.S.A. (e-mail: aschwanden@lmsal.com)*

(Received 19 July 2002; accepted 15 August 2002)

Abstract. We obtain a theoretical description of the height (z) distribution of flare hard X-rays in the collisional thick-target model as a function of photon energy ε. This depends on the target atmosphere density structure $n(z)$ and on the beam spectral index δ. We show that by representing the data in terms of the 1-D function $z_{\max}(\varepsilon)$ defining where the emission peaks as a function of ε it is possible to derive $n(z)$ from data on $z_{\max}(\varepsilon)$. This is done first on the basis of a simple stopping depth argument then refined to allow for the dependence on spectral index δ. The latter is worked out in detail for the case of a parameterization $n(z) = n_0\ (z/z_0)^{-b}$ which yields numerical results for $z_{\max}(\varepsilon)$ well fit by $z_{\max}(\varepsilon) \sim \varepsilon^{-\alpha}$, with α dependent on δ, which is also found to fit well to actual observations. This enables derivation of flare loop $n(z)$ in terms of n_0, b from RHESSI data in an entirely novel way, independent of other density diagnostic methods, and also of how $n(z)$ varies with time in flares such as by evaporation, as detailed in companion Paper II.

1. Introduction

The spatial distribution of energy loss in solar flares can provide us with vital information on the origin and propagation of accelerated nonthermal particles, which carry a significant amount of the energy released in flares. Today we assume that in most flares the particle acceleration site is located in coronal magnetic reconnection sites, where the plasma is nearly collisionless. The accelerated particles propagate along the newly-reconnected field lines, either downward toward the chromosphere, or upward along large-scale loops or open field lines. The downward propagating electrons reach the chromosphere either directly, if they have sufficiently small pitch angles, or after some intermediate trapping with subsequent precipitation, in the case of large pitch angles. The overall scenario seems to hold for most flare observations (for a review see Aschwanden, 2002). A major new aspect of the present study is use of the high-energy resolution of RHESSI to measure the energy loss as function of height with high precision, which can be used for reconstruction of the chromospheric density profile, if we assume collisional losses only. Since the observed nonthermal hard X-ray emission is a direct result of energetic beam electrons, we can probe the density locally in regions where fast

Solar Physics **210:** 373–381, 2002.

electrons interact with a dense target. Most other chromospheric density modeling is based on line-of-sight integrated EUV line emission that contain contributions from a very long path through an inhomogeneous solar atmosphere, and thus are subject to unknown filling factors. Moreover, X-rays are least affected by propagation effects, unlike radio emission that is generated by the same electrons and can be strongly affected by the plasma where electromagnetic waves propagate.

In this paper we derive the relevant theory in terms of the thick-target model, while the data analysis for the case of the 20 February 2002 flare is presented in a companion paper (Aschwanden, Brown, and Kontar, 2002, Paper II).

2. Theory

The aim of this study is to show that one can infer a source plasma density structure $n(z)$ from hard X-ray source height data obtained by RHESSI, assuming a purely collisional thick-target model (Brown, 1971), and to see whether this $n(z)$ is consistent with the results from other data. The underlying theory has been previously developed by calculations of the thick-target model height structure (Brown and McClymont, 1976; Emslie and Vlahos, 1980) based on treatments of the collisional transport (Brown, 1972, 1973; Emslie, 1978; Brown *et al.*, 1983) but we re-derive it here to suit our specific application.

2.1. Simplifying assumptions

In previous work, the following simplifying assumptions have been made as a first approximation of the problem: (1) full target ionization , (2) one-dimensional Coulomb collisional transport, neglecting pitch-angle changes (pitch angle $\alpha = 0$ or $\mu = \cos\alpha = 1$), (3) no mirroring of particles, and (4) power-law function for electron injection flux energy spectrum. As in Brown (1971), $F_0(E_0)$ is the flux spectrum of injected electrons, while $F(E, N)$ denotes the instantaneous electron flux spectrum at a column depth $N(z)$, and $n(z)$ denotes the local number density of the ambient plasma. The height z refers to the altitude above some reference level, such as the photosphere. The acceleration site is assumed to be localized, somewhere in the corona where collisional energy loss is negligible (in the framework of the thick-target model). To avoid complicating geometric projection effects, we concentrate here only on limb flares, where flare loops are viewed side-on, without (appreciable) projection effects. The collisional thick-target region of interest is located close to the flare loop footpoints, so that this loop segment can be approximated with a vertical flux tube.

2.2. COLLISIONAL TRANSPORT

Collisional transport gives, in the limit of zero pitch angle ($\mu = 1$) and neglecting pitch angle scattering, the following dependence of the kinetic electron energy E as function of the column depth $N(z) = \int_z^{z_{\max}} n(z')\,\mathrm{d}z'$ as in Brown (1972):

$$E(E_0, N) = (E_0^2 - 2KN)^{1/2}\,, \tag{1}$$

which defines the following stopping depth N_s for energy E_0,

$$N_s(E_0) = \frac{E_0^2}{2K}\,, \tag{2}$$

where $K = 2\pi e^4 \Lambda$ is a constant with Λ the Coulomb logarithm (see Spitzer, 1962).

The continuity condition then yields (using Equation (1))

$$F(E, N) = F_0(E_0)\frac{\mathrm{d}E_0}{\mathrm{d}E} = F_0([E^2 + 2KN]^{1/2})\frac{E}{(E^2 + 2KN)^{1/2}} \tag{3}$$

for the local electron spectrum $F(E, N)$ as a function of N. Note that we neglect here the fact that Λ may vary somewhat in lower regions where the ionization falls (e.g., Emslie, 1978).

2.3. SIMPLE TREATMENT

For a steep electron spectrum, bremsstrahlung photons with energy ε are mainly produced by electrons of energy $E \approx \varepsilon$. Such electrons typically stop at a depth with column density N_s given by Equation (2),

$$N_s(\varepsilon) \approx \frac{\varepsilon^2}{2K}\,. \tag{4}$$

So, ignoring the spectral dependence for now, we roughly expect to see photons of energy ε from height z around

$$z(\varepsilon) = z\left(N = N_s(\varepsilon) = \frac{\varepsilon^2}{2K}\right) \tag{5}$$

(but see Section 2.4 below for more accurate analysis). If the centroid of flare loop footpoint sources at energies ε is observed with RHESSI to occur at height $z(\varepsilon)$, then we can estimate the source height dependence of the column depth $N(z)$ by equating Equation (5) to the data values, i.e.,

$$N(z) = \frac{\varepsilon^2(z)}{2K}. \tag{6}$$

This $N(z)$ defines the atmospheric structure required for the data to be consistent with the collisional thick-target model. To obtain the chromospheric density $n(z)$ we take the derivative $\mathrm{d}/\mathrm{d}z$ of Equation (6),

$$n(z) = -\frac{\mathrm{d}N(z)}{\mathrm{d}z} = -\frac{\varepsilon}{K}\frac{\mathrm{d}\varepsilon}{\mathrm{d}z}\,. \tag{7}$$

For real measurements at discrete energy values ε_1 and ε_2 we can express the derivative by

$$n(z) \approx \frac{(\varepsilon_1+\varepsilon_2)}{2K}\frac{\varepsilon_2-\varepsilon_1}{z_1-z_2} = \frac{1}{2K}\frac{\varepsilon_2^2-\varepsilon_1^2}{(z_1-z_2)}. \tag{8}$$

In terms of numerical values we use a Coulomb logarithm of $\Lambda \approx 20$, so that $K = 2\pi e^4\Lambda \approx 6.7\times10^{-36}$ (erg cm)^2, yielding

$$N(z) \approx 10^{20}\ \mathrm{cm}^{-2}\left(\frac{\varepsilon_2}{20\ \mathrm{keV}}\right)^2, \tag{9}$$

$$n_e \approx 10^{12}\ \mathrm{cm}^{-3}\frac{(\varepsilon_2/20\ \mathrm{keV})^2-(\varepsilon_1/20\ \mathrm{keV})^2}{(z_1/1000\ \mathrm{km})-(z_2/1000\ \mathrm{km})}\,. \tag{10}$$

2.4. Exact expression with spectral dependence

The photon flux per unit energy ε per unit source height range dz at Earth distance D is, for a bremsstrahlung cross-section $Q(\varepsilon, E)$ and beam area A,

$$\frac{\mathrm{d}I}{\mathrm{d}z}(\varepsilon,z) = \frac{A}{4\pi D^2}n(z)\int_\varepsilon^\infty F(E,N)Q(\varepsilon,E)\,\mathrm{d}E \qquad (\mathrm{cm}^{-2}\ \mathrm{s}^{-1}\ \mathrm{erg}^{-1}\ \mathrm{cm}^{-1})\,. \tag{11}$$

We use Kramer's cross-section

$$Q(\varepsilon,E) = \frac{Q_0 m_e c^2}{\varepsilon E}, \tag{12}$$

where Q_0 is as in Brown and Emslie (1988) and approximate the injection spectrum $F_0(E_0)$ with a power-law function,

$$F_0(E_0) = (\delta-1)\frac{F_1}{E_1}\left(\frac{E_0}{E_1}\right)^{-\delta}\,. \tag{13}$$

Using Equations (3) and (1), Equation (11) becomes with Equation (12)

$$\frac{\mathrm{d}I}{\mathrm{d}z}(\varepsilon,z) = \frac{AQ_0}{4\pi D^2}\frac{m_e c^2}{\varepsilon}n(z)\int_\varepsilon^\infty \frac{F_0((E^2+2KN)^{1/2})}{(E^2+2KN)^{1/2}}\,\mathrm{d}E \tag{14}$$

and for a power-law injection function (14) is

$$\frac{\mathrm{d}I_\varepsilon}{\mathrm{d}z} = (\delta-1)\frac{AF_1}{E_1^{\delta+1}}\frac{Q_0}{4\pi D^2}\frac{m_e c^2}{\varepsilon}n(z)\int_\varepsilon^\infty \frac{\mathrm{d}E}{(E^2+2KN)^{(\delta+1)/2}}. \tag{15}$$

The product $AF_1 = \mathcal{F}_1$ is the total flux of electrons s^{-1} at $E_0 \geq E_1$ over the area A. Introducing $u(\varepsilon, z) = \varepsilon^2/2KN(z)$, one immediately obtains

$$\frac{dI}{dz}(\varepsilon, z) = (\delta - 1)\frac{\mathcal{F}_1}{E_1}\frac{Q_0}{8\pi D^2}\frac{m_e c^2}{\varepsilon}n(z)\left(\frac{2KN}{E_1^2}\right)^{-\delta/2} B\left(\frac{1}{1+u}, \frac{\delta}{2}, \frac{1}{2}\right), \tag{16}$$

where B is an incomplete Beta function,

$$B\left(\frac{1}{1+u}, \frac{\delta}{2}, \frac{1}{2}\right) \equiv \int_0^{1/(1+u)} x^{\delta/2-1}(1-x)^{-1/2}\, dx. \tag{17}$$

Note that the incomplete beta function B (Equation (17)) depends on ε only in the combination $u = \varepsilon^2/2KN$, which is similar to the expression considered in Section 2.3 above. On the other hand, $n(z)[2KN/E_1^2]^{-\delta/2}$ depends only on z for a given δ, and is independent of ε.

2.5. Peak of $dI/dz(\varepsilon, z)$ for power-law density model $n(z)$

Based on the argument of the stopping depth $N(\varepsilon)$,

$$N(\varepsilon) \approx \frac{\varepsilon^2(z)}{2K}, \tag{18}$$

we found from data fitting that the energy dependency $\varepsilon(z)$ can be approximated by a power-law function (see Paper II), that immediately brings us the density power law via Equation (18). Therefore, we assume that

$$n(z) = n_0\left(\frac{z}{z_0}\right)^{-b}, \tag{19}$$

so that the column depth $N(z)$ becomes

$$N(z) = \int_z^\infty n(z)\, dz = N_0\left(\frac{z}{z_0}\right)^{1-b}, \tag{20}$$

where

$$N_0 = \frac{n_0 z_0}{b-1}. \tag{21}$$

The upper limit of the column depth integral is approximated with $z_{\max} \approx \infty$, which is saying essentially that the beam encounters little material before it reaches the chromosphere, so that $z \ll z_{\max}$.

The proposal is now to see how well we can fit the data on $z(\varepsilon)$ from gaussian models of RHESSI data to the predictions of dI/dz (ε, z) in the previous theory framework (Equation (16)), but using a chromospheric model of $n(z)$ and $N(z)$ defined in terms of power laws like (Equations (19) and (20)), estimated from the

simple model approach but now adjusting the parameters (b, n_0) to take account of the spectral dependence of the peak emission heights.

Inserting the chromospheric density model (Equations (19) and (20)) into Equation (16) gives

$$\frac{\mathrm{d}I}{\mathrm{d}z}(\varepsilon, z) = I_0 \frac{\sqrt{2KN_0}}{\varepsilon} \left(\frac{z}{z_0}\right)^{-b+(b-1)\delta/2} B\left(\frac{1}{1+\dfrac{\varepsilon^2}{2KN_0}\left(\dfrac{z}{z_0}\right)^{b-1}}, \frac{\delta}{2}, \frac{1}{2}\right), \quad (22)$$

where I_0 is just a flux scale factor,

$$I_0 = (\delta - 1)\frac{\mathcal{F}_1}{E_1}\frac{Q_0}{8\pi D^2}\frac{m_e c^2}{\sqrt{2KN_0}} n_0 \left(\frac{2KN_0}{E_1^2}\right)^{-\delta/2} \quad (23)$$

independent of the altitude z and the photon energy ε.

What we want to find out is where Equation (22) peaks in z for each ε. This will depend on the spectral slope δ, the reference height z_0, and the parameters b, N_0 defining the atmosphere model. We can consider the shape of Equation (22) in terms of the dimensionless parameters $\tilde{\varepsilon} = (\varepsilon/\varepsilon_0)$ and $\tilde{z} = (z/z_0)$, by defining the reference energy ε_0 via Equation (4),

$$\varepsilon_0 = \sqrt{2KN_0}\,, \quad (24)$$

which yields the dimensionless form of Equation (22),

$$\frac{\mathrm{d}I}{\mathrm{d}z}(\tilde{\varepsilon}, \tilde{z}) = I_0\, \tilde{\varepsilon}^{-1} \tilde{z}^{-b+(b-1)\delta/2}\, B\left(\frac{1}{1+\tilde{\varepsilon}^2\tilde{z}^{b-1}}, \frac{\delta}{2}, \frac{1}{2}\right). \quad (25)$$

For a given chromospheric model (with free parameters n_0, b, with $N_0 = n_0 z_0/(b-1)$), an arbitrary reference height z_0, and an electron spectrum slope δ, we can numerically determine the surface $\mathrm{d}I/\mathrm{d}z\ (\tilde{\varepsilon}, \tilde{z})$ in dimensionless parameter space $(\tilde{\varepsilon}, \tilde{z})$ and find the maximum $\tilde{z}_{\max}(\tilde{\varepsilon})$ as a function of photon energy $\tilde{\varepsilon}$. The independent parameters (n_0, b) can then be varied until a best fit of the model (Equation (25)) to the observed height dependence $\tilde{z}^{\mathrm{obs}}_{\max}(\tilde{\varepsilon})$ is obtained.

The spatial distribution of the flux $\mathrm{d}I/\mathrm{d}z\ (\varepsilon, z)$ is shown in Figures 1 and 2. We calculated examples of this function for a density power-law parameter of $b = 2.5$ in the chromospheric model, a spectral slope of $\gamma = 4.0$ of the photon spectrum (appropriate to Paper II), and by varying the energy $\varepsilon = 10, \ldots, 60$ keV (Figure 1). The spectral dependence of the peak height is shown for the same density power-law parameter $b = 2.5$, a photon energy of $\varepsilon = 20$ keV, and by varying the spectral slope in the range of $\delta = 2.5, \ldots, 5.0$ (Figure 2). Note the strong spectral dependence of the peak emission height $z_{\max}(\varepsilon)/z_0$. The flux profiles in Figure 2 show clearly that the radiation is spread mainly along the upper loop for soft spectra ($\delta = 6.0$), because the majority of low-energy electrons are not able to penetrate to the dense chromosphere before they lose their energy, while harder

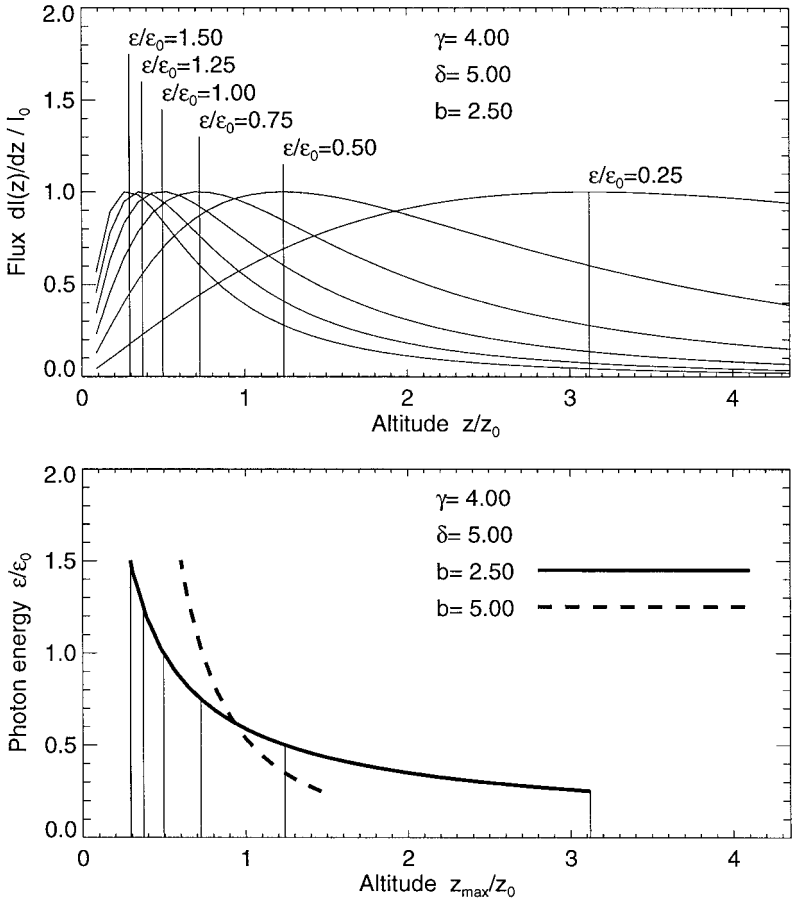

.

Figure 1. The analytical functions of the energy flux per height range, $dI/dz\ (\varepsilon, z)$ (see Equation (25)), for six different energies, $\varepsilon = 10, 20, \ldots, 60$ keV, as function of the dimensionless altitude z/z_0 (*top panel*). The functions are calculated for $b = 2.5$, $\gamma = 4.0$, and are normalized to unity. The locations of the maximum of these functions, $z_{\max}(\varepsilon)/z_0$, are found numerically (*bottom panel*).

spectra ($\delta = 3.5$) contain a larger fraction of high-energy electrons that propagate all the way to the dense chromosphere, yielding maximum radiation at heights of $z_{\max}/z_0 \lesssim 1$ (Figure 2, top).

3. Discussion and Conclusions

We see from Equation (10) how data on $z_{\max}(\varepsilon)$ can yield estimates of the atmospheric density structure $n(z)$ from hard X-ray spectral images. Using the more refined treatment allowing for spectral index δ dependence shows (Figure 1) how

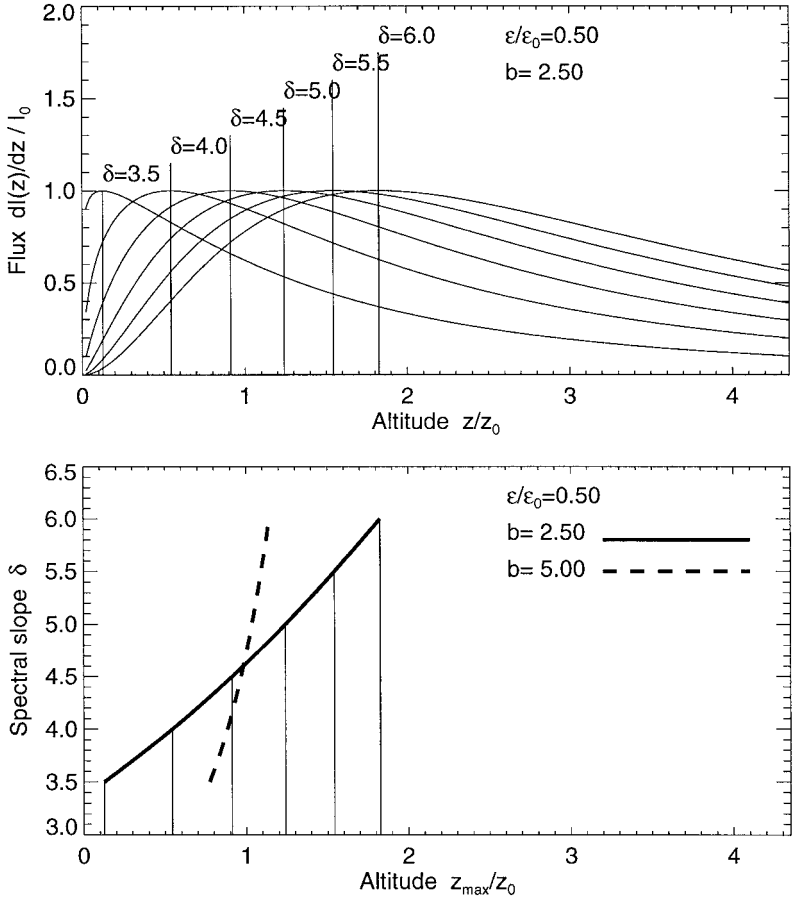

Figure 2. The spectral dependence of the analytical function $\mathrm{d}I/\mathrm{d}z\ (\varepsilon, z)$ (see Equation (25)) is shown for six different spectral slopes $\gamma = 2.5, \ldots, 5.0$ of the photon spectrum (i.e., $\delta = 3.5, \ldots, 6.0$). The spatial distribution of the fluxes are shown as function of the the dimensionless altitude z/z_0 (*top panel*), and the maxima $z_{\max}(\varepsilon)/z_0$ have been calculated numerically (*bottom panel*).

the peak emission altitude $z_{\max}(\varepsilon)$ depends monotonically, for given δ, on the values of the parameters n_0, b in our (power-law) parameterized model of $n(z)$ and hence enables their inference from data as shown for RHESSI observations in Paper II. There we also discuss the effect of relaxing simplifying assumptions in our theoretical treatment of the thick-target model and how our resulting $n(z)$ compares with results from other density diagnostic methods.

Some specific simplifying assumptions we have made can also affect the results. In particular we used a 1-D treatment of the transport, ignoring pitch angle increase, and assumed zero injection pitch angle. These assumptions were relaxed in Brown (1972) from which it is easy to see that their inclusion would have the qualitative effect of an increase by a factor ≥ 1.5 in the collisional transport K value and hence a decrease in the inferred values of $N(z), n(z)$ for given height structure

data. Secondly in K we used $\Lambda = \Lambda_{ee}$ for an ionized target rather than $\Lambda = \Lambda_{eH}$ for a neutral one which is smaller by a factor of about 0.4 and hence will make inferred $N(z), n(z)$ values larger by a factor of about 2.5. Ignoring return current losses will also tend to make estimated $N(z), n(z)$ too large. Clearly if the fullest use is to be made of the hard X-ray method of measuring densities and studying energy loss process the more fully these effects can be included the better, though our results seem to prove that the basic ionized target collisional thick-target model is good within factors of a few and so an excellent starting point.

Acknowledgements

Support for this work was provided by the NASA SMEX grant NAS5-98033 through University of California, Berkeley (subcontract SA2241-26308PG) and by UK PPARC Standard and Visitor Grants.

References

Aschwanden, M. J.: 2002, *Space Sci. Rev.* **101**, 240.
Aschwanden, M. J., Brown, J. C., and Kontar, E. P.: 2002, *Solar Phys.*, this volume, Paper II.
Brown, J. C.: 1971, *Solar Phys.* **18**, 489.
Brown, J. C.: 1972, *Solar Phys.* **26**, 441.
Brown, J. C.: 1973, *Solar Phys.* **32**, 227.
Brown, J. C. and MacKinnon, A. L.: 1985, *Astrophys. J.* **292**, L3l.
Brown, J. C. and Emslie, A. G.: 1988, *Astrophys. J.* **331**, 554.
Brown, J. C. and McClymont, A. N.: 1976, *Solar Phys.* **49**, 329.
Brown, J. C., Carlaw, V. A., Cromwell, D., and Kane, S. R.: 1983, *Solar Phys.* **88**, 281.
Emslie, G. A.: 1978, *Astrophys. J.* **224**, 241.
Emslie, G. A. and Vlahos, L.: 1980, *Astrophys. J.* **242**, 359.
Spitzer, L. W.: 1962, *Physics of Fully Ionized Gases*, 2nd ed., Interscience, New York.